

Crossed Molecular Beam Study on the Ground State Reaction of Atomic Boron [B(²P_j)] with Hydrogen Cyanide [HCN(X¹Σ⁺)]

Brant Jones,^{†,‡} Pavlo Matsyutenko,[†] Nung C. Su, Agnes H. H. Chang,[§] and Ralf I. Kaiser^{*†}

Department of Chemistry, University of Hawaii at Manoa, Honolulu, Hawaii 96822, USA, NASA Astrobiology Institute, University of Hawaii at Manoa, Honolulu, Hawaii 96822, USA, and Department of Chemistry, National Dong Hwa University, Shoufeng, Hualien 974, Taiwan

Received: May 14, 2010; Revised Manuscript Received: July 8, 2010

The linear boronisocyanide species, [BNC(X¹Σ⁺)], represents the simplest triatomic molecule with three distinct, neighboring main group atoms of the second row of the periodic table of the elements: boron, carbon, and nitrogen. This makes boronisocyanide a crucial benchmark system to understand the chemical bonding and the electronic structure of small molecules, in particular when compared to the isoelectronic tricarbon molecule, [CCC(X¹Σ_g⁺)]. However, a clean, directed synthesis of boronisocyanide—a crucial prerequisite to study the properties of this molecule—has remained elusive so far. Here, we combine crossed molecular beam experiments of ground state boron atoms (²P_j) with hydrogen cyanide with electronic structure calculations and reveal that the boronisocyanide molecule, [BNC(X¹Σ⁺)], is formed as the exclusive product under gas phase single collision conditions. We also show that higher energy isomers such as the hitherto unnoticed, ring-strained cyclic BNC(X³A′) structure, which is isoelectronic to the triplet, cyclic tricarbon molecule, [C₃(X³A₂′)], do exist as local minima. Our studies present the first directed synthesis and observation of gas phase boronisocyanide providing a doorway for further fundamental studies on one of the simplest triatomic molecules composed solely of group III–V elements.

1. Introduction

Small boron-bearing molecules have attracted substantial interest from the chemistry community^{1–8} to better rationalize basic concepts of molecular structure^{9–13} and chemical bonding.^{14–22} The boronisocyanide molecule, BNC, presents the simplest triatomic molecule holding three distinct, neighboring main group atoms of the second row of the periodic table of the elements. These are boron (B; group III), carbon (C; group IV), and nitrogen (N; group V). Following Langmuir's fundamental isoelectronic concept,^{23,24} it is easy to rationalize that boronisocyanide is isoelectronic to the linear tricarbon molecule (CCC; C₃), in which the boron and nitrogen atoms with three and five valence electrons, respectively, are formally replaced by two carbon atoms with four valence electrons each. This fundamental periodic property is expected to translate into similar electronic characteristics of boronisocyanide and tricarbon. Here, both molecules are closed shell species, are linear in nature, and belong to the *C_{∞v}* and *D_{∞h}* point groups, respectively (Figure 1, Table 1). This is also reflected in the ¹Σ⁺ and ¹Σ_g⁺ electronic ground states of boronisocyanide and tricarbon, respectively, differing only by the parity due to the lack of an inversion center in boronisocyanide. The linear isomers [BCN(X¹Σ⁺)] and [CBN(X¹Σ⁺)] are 53 and 330 kJ mol⁻¹ less stable than boronisocyanide, respectively.^{25,26} Also, tricarbon and boronisocyanide both have high-energy cyclic isomers, which lie about 82–97 kJ mol⁻¹ and 169 kJ mol⁻¹ (as determined in this work) above the thermodynamically most stable linear structure.^{27,28} However, the cyclic structures have been only characterized

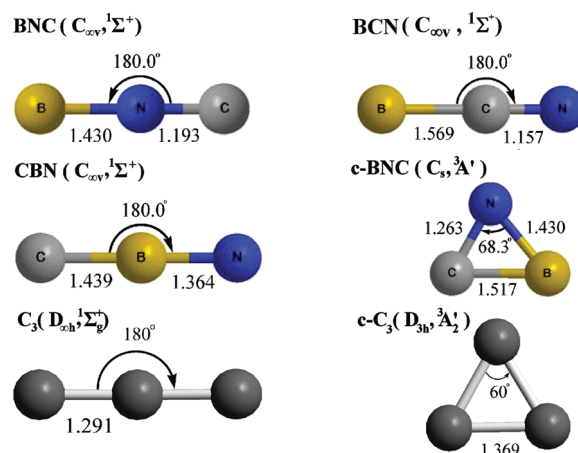


Figure 1. Optimized geometries of distinct isomers of BNC and CCC as compiled in Table 1. Bond lengths are in units of angstroms (Å). Geometries for the CCC isomers are taken from ref 27. The geometries of BNC isomers are derived from this work. The colors yellow, blue, and gray represent boron, nitrogen, and carbon, respectively.

theoretically and were found to have triplet ³A₂′ and ³A′ electronic ground states, respectively. The lowest singlet states were first order transition states connecting to the linear isomers.

Besides this fundamental interest of the BNC molecule in chemical bonding and electronic structure, ternary boron-nitrogen-carbon containing compounds have gained significant attention due to their unusual physical and chemical characteristics. First, BNC nanostructures have been shown to have higher than predicted chemical and thermal stabilities than their analogous carbon nanostructures.^{29–36} This brings important technological applications of BNC material as oxygen-resistant coatings for carbon fiber materials^{37,38} as high temperature transistors, electrical conductors, and lubricants.³⁹ Furthermore,

* To whom correspondence should be addressed. E-mail: ralfk@hawaii.edu.

[†] Department of Chemistry, University of Hawaii at Manoa.

[‡] NASA Astrobiology Institute, University of Hawaii at Manoa.

[§] Department of Chemistry, National Dong Hwa University.

TABLE 1: Compilation of Energetics, Electronic Ground State, Point Groups, and Vibrational Frequencies of BNC and CCC Isomers

molecule	relative energy (kJ mol ⁻¹)	electronic ground state	point group	vibrational frequencies (cm ⁻¹)
¹¹ BNC	0 ^{25,26a} 40 ²⁵	1Σ ⁺	C _{∞v}	2075.98, 140.16, 991.01; ²⁵ 2055.2, n/o, 984.3 ²⁶
¹¹ BCN	54 ²⁶ 42 ^a	1Σ ⁺	C _{∞v}	2165.52, 203.82, 809.87; ²⁵ 2170.8, n/o, 800.0 ²⁶
C ¹¹ BN	330 ²⁶ 346 ^a	1Σ ⁺	C _{∞v}	1964.3, 128.1, 983.3 ²⁶
c-BCN	169 ^a	3A'	C _s	<i>a'</i> – 1127.1, 1657.5; <i>a''</i> – 830.2 ^a
C ₃	0 ²⁵	1Σ _g ⁺	D _{∞h}	2045.31, 44.12, 1214.34; ²⁵ 2040.02, 63.42, 1226.6 ⁶⁶
c-C ₃	82 ²⁸ 97 ²⁷	3A' ₂	D _{3h}	<i>e'</i> – 1155 <i>a'</i> ₁ – 1618 ²⁸

^a This work. n/o = not observed; italics designates ab initio calculations.

BNC nanotubes have the asset of being electrically luminescent with applications for flat panel displays.⁴⁰ Amorphous BNC films also have the unique optical advantage of being highly transparent in the X-ray portion of the electromagnetic spectrum from 10 to 0.1 nm (124–12 400 eV); therefore, these structures can be utilized as optical masks for X-ray lithography.⁴¹ Recently, a computational investigation has revealed that carbon-doped boron nitride cages can achieve a high hydrogen storage amount of up to 7.43% in weight; the dehydrogenation of the corresponding BNC hydrides is thermodynamically favorable, making the BNC cages a highly competitive candidate for hydrogen storage material.⁴² Second, the BNC molecule is also relevant to more exotic research areas such as astrochemistry and the chemical evolution of the interstellar medium. Here, boron has been detected toward the Orion association,⁴³ specifically λ Ori, κ Ori, and ι Ori with column densities of 6.17, 4.26, and ≤ 1.99 × 10¹⁰ cm⁻².^{44–48} The potential precursor to the BCN molecule, hydrogen cyanide (HCN), was also monitored in the Orion KL nebula with a column density of 2.6 × 10¹⁶ cm⁻².⁴⁹ Here, a reaction of atomic boron with hydrogen cyanide might lead to the BNC molecule with the emission of atomic hydrogen.

However, despite successful “bulk” preparation of BNC material by arc-methods,^{50–53} laser ablation,^{26,54–56} chemical vapor deposition,^{57–63} and radio frequency magnetron sputtering,^{64,65} the characterization of its simplest triatomic precursor, boronisocyanide (BNC), has proven challenging. Lanzisera et al. conducted the only experimental study so far utilizing matrix isolation of BNC(X¹Σ⁺) and BCN(X¹Σ⁺) formed in the plume of laser ablated boron atoms with hydrogen cyanide at 6–10 K.²⁶ Nevertheless, no directed synthesis has been elucidated to prepare the boronisocyanide in the gas phase. A preparation of boronisocyanide under *controlled conditions* in the gas phase would pave the way for future investigations in the microwave and infrared regime and, hence, would lead to an understanding of the electronic properties of boronisocyanide. The knowledge gained from these gas phase spectroscopic studies is crucial and can be compared directly with ab initio electronic structure calculations and further used as a benchmark for the validity of these calculations for one of the simplest triatomic molecule formed from three distinct neighboring second row elements of the periodic table: boronisocyanide (BNC).

Here, we report on the very first gas phase synthesis of the boronisocyanide molecule utilizing the crossed molecular beam

approach by crossing a supersonic beam of ground state boron atoms with a beam of hydrogen cyanide molecules. This represents a prototype reaction of the simplest Lewis acids (the electron-deficient boron atom holds a ²P electronic ground state and a (1s)²(2s)²(2p)¹ electron configuration) with one of the simplest Lewis bases (the triatomic hydrogen cyanide molecule). The experimental studies are complemented with high level electronic structure calculations to compare the experimental findings with theoretical predictions.

2. Experimental and Data Analysis

The experiments were conducted in a universal crossed molecular beam machine under single collision conditions at The University of Hawaii.^{67–69} Briefly, a supersonic beam of ¹¹B(²P_j) atoms was generated in the primary source via laser ablation of boron at 266 nm by focusing the 30 Hz, 5–7 mJ per pulse output of a Spectra-Physics PRO-270-30 Nd:YAG laser onto a rotating boron rod (Alfa Aesar, 99.9%).⁷⁰ The ablated species were subsequently seeded into helium carrier gas released by a Proch–Trickl valve⁷¹ operating with a 0.5 mm nozzle at 60 Hz, 80 μs pulse width, –500 V pulse amplitude, and 4 atm backing pressure. Under these operating conditions, the pressure in the primary source was maintained at about 9 × 10⁻⁵ Torr. After passing a skimmer, a four-slot chopper wheel selected a part of the atomic boron (¹¹B) beam with a peak velocity (*v_p*) of 2210 ± 50 ms⁻¹ and a speed ratio (*S*) of 3.5 ± 0.3. The integrated time-of-flight (TOF) spectra at *m/z* = 10 (¹⁰B⁺) and *m/z* = 11 (¹¹B⁺) reflected the natural isotopic abundance ratio of 20% ¹⁰B and 80% ¹¹B. This segment of the atomic boron [¹¹B(²P_j)] beam crossed a pulsed hydrogen cyanide (HCN) beam originating from the secondary source. A certified mixture (4.5 ± 2.0%) hydrogen cyanide in helium (Matheson Tri-Gas) was released from a second Proch–Trickl pulsed valve 20 μs prior to the primary valve operated with a 1.0 mm nozzle at 60 Hz, 80 μs pulse width, –500 V pulse amplitude, and 600 Torr backing pressure to cross the ¹¹B (²P_j) atomic beam perpendicularly in the interaction region. The distance between the nozzle tip and skimmer was about 14 mm. The peak velocity (*v_p*) and speed ratio (*S*) of the hydrogen cyanide beam were determined to be 1610 ± 20 ms⁻¹ and 26.1 ± 1.9, respectively. This resulted in a collision energy of 29.2

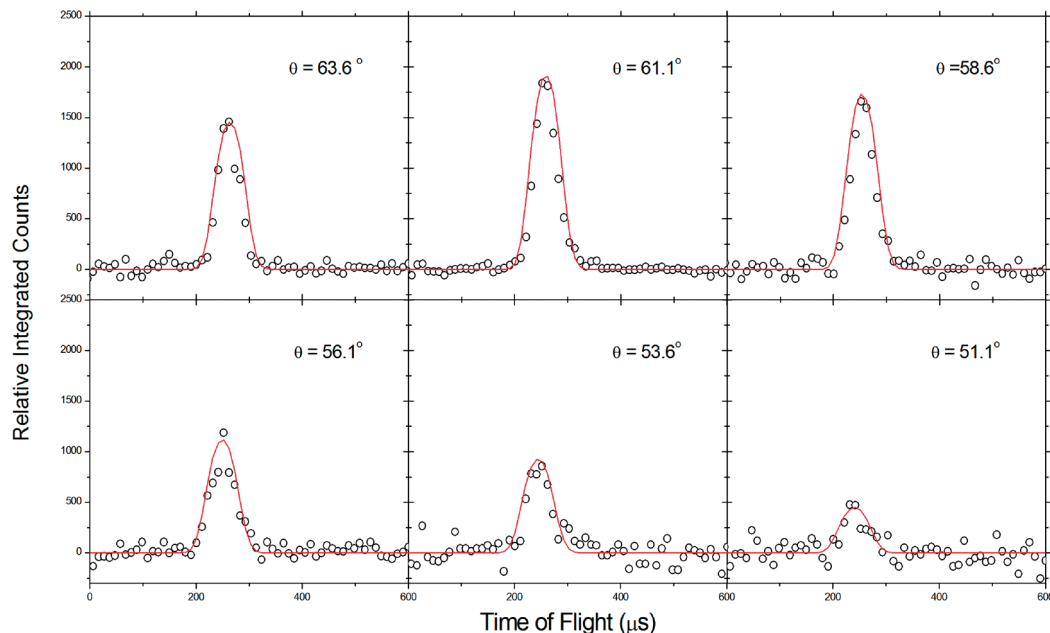


Figure 2. Time-of-flight spectra of the ionized reaction product monitored at $m/z = 37$ ($^{11}\text{BNC}^+$) formed in the reaction of $^{11}\text{B}(^2\text{P}_j)$ with hydrogen cyanide [$\text{HCN}(X^1\Sigma^+)$]. Open circles signify the experimental data. Solid red lines represent the calculated distribution of the boronisocyanide (BNC) product.

$\pm 1.5 \text{ kJ mol}^{-1}$. During operation of the secondary pulsed valve, the pressure in the secondary chamber was typically at 1×10^{-5} Torr.

The reactively scattered products were monitored by a triply differentially pumped quadrupole mass spectrometric detector operated in the time-of-flight (TOF) mode after electron impact ionization of the molecules at 80 eV with an emission current of 2 mA. These ionized neutrals were then mass separated by an Extrel QC 150 quadrupole mass spectrometer operated with an oscillator at 2.1 MHz; only ions with a desired m/z value passed through and were accelerated toward a stainless steel target coated with an aluminum layer and operated at a voltage of -22.5 kV . The ions hit the surface and initiated an electron cascade that was accelerated under the same potential until they reached an aluminum coated organic scintillator whose photon cascade was detected by a photomultiplier tube (PMT, Burle, Model 8850) operated at -1.35 kV . The signal from the PMT was then filtered by a discriminator (Advanced Research Instruments, Model F-100TD) at a level of 1.4 mV prior to directing into a Stanford Research System SR430 Multi-Channel Scaler to record the TOF spectra. The detector is rotatable within the plane as defined by the boron and hydrogen cyanide beams. Up to 2.6×10^6 TOF spectra were recorded at each angle. The laboratory angular distribution was acquired by integration of the TOF spectra at each collection angle and normalizing for the accumulation time and fluctuations in the boron beam intensity. To gain additional information on the chemical dynamics and underlying reaction mechanism, TOF spectra and the laboratory angular distribution were fit and transformed into the center-of-mass reference frame using a forward-convolution routine.^{72,73} This approach initially presumes an angular flux distribution $T(\theta)$ and translational energy flux distribution $P(E_T)$ in the center-of-mass system assuming mutual independence. The laboratory data (TOF spectra and laboratory angular distribution) are then calculated from the $T(\theta)$ and $P(E_T)$ and convoluted over the apparatus functions to obtain a simulation of the experimental data. The crucial output of this fitting routine is the product flux contour map, $I(\theta, u) = P(u) \times T(\theta)$, which plots the intensity of the reactively scattered products (I) as a

function of the center-of-mass scattering angle (θ) and product velocity (u). This plot is called the reactive differential cross section and can be seen as the image of the chemical reaction. The energy dependence on the cross section was not hypercritical in the overall global fit employed using the forward convolution technique. Utilizing the energy dependent cross section, $\sigma(E_c) \approx (1 - E_c/E_0)$, based upon the line of centers model⁷⁴ with the collision energy (E_c) for $E_c \geq E_0$, we could fit the data with energy thresholds, E_0 , between 6 kJ mol^{-1} and 10 kJ mol^{-1} .

3. Electronic Structure Calculations

The dynamic pathways pertaining to the reaction of ground state boron atoms [$\text{B}(^2\text{P}_j)$] with hydrogen cyanide [$\text{HCN}(X^1\Sigma^+)$] on the adiabatic, ground state doublet surface were investigated computationally via ab initio principles. Three initial collision complexes were identified. Subsequently, probable low-energy isomerization and dissociation channels for each collision complex were searched for and characterized; these included hydrogen shifts, ring closure and opening, as well as hydrogen loss pathways. The optimized geometries and harmonic frequencies of the intermediates, transition states, and dissociation products were obtained at the level of the hybrid density functional theory, the unrestricted B3LYP/cc-pVTZ.^{75–78} The energies were then refined at the coupled cluster CCSD(T)/cc-pVDZ level with B3LYP/cc-pVTZ zero-point energy corrections.^{79–82} The Gaussian03 program was employed in the electronic structure calculations.⁸³ Our calculations are accurate within $\pm 4 \text{ kJ mol}^{-1}$.

4. Experimental Results

4.1. Laboratory Data. Reactive scattering signal for the reaction of atomic boron, $^{11}\text{B}(^2\text{P}_j)$, with hydrogen cyanide, $\text{HCN}(X^1\Sigma^+)$, was monitored at $m/z = 37$ ($^{11}\text{BNC}^+$). These ions correspond to the parent ions and present the most intense mass fragment. Due to the high background level at $m/z = 12$ from the detector background, no discernible signal was detected from the hydrogen abstraction reaction to form the ^{11}BH radical plus

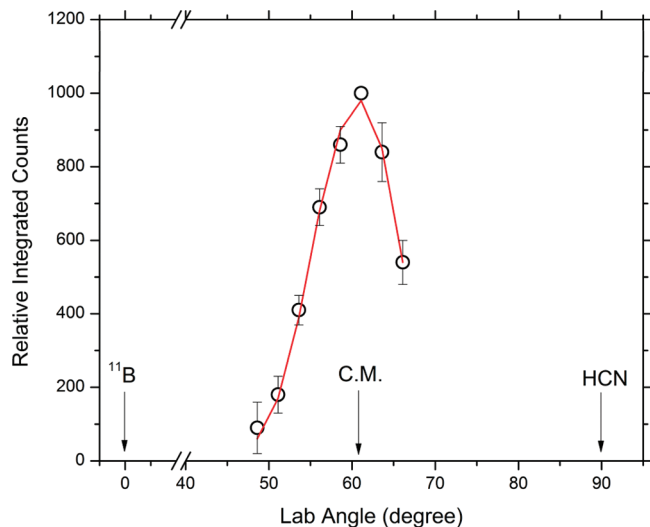


Figure 3. Laboratory angular distribution for the reaction of $^{11}\text{B}(^2\text{P}_j)$ with hydrogen cyanide [$\text{HCN}(X^1\Sigma^+)$]; the product was monitored at $m/z = 37$ ($^{11}\text{BNC}^+$). Open circles represent the experimental data together with 1σ error bars. The solid red line corresponds to the calculated distribution for the ^{11}BNC product; C.M. designates the center-of-mass angle.

the cyano radical (CN). Similarly, TOF spectra were not collected at lower m/z values as a consequence of the high background from the secondary reactant beam in conjunction with the mass fragmentation of the hydrogen cyanide reactant. However, based on energetics from the NIST database,⁸⁴ the hydrogen abstraction channel is highly endoergic by about 178 kJ mol^{-1} ; considering our collision energy of 29.2 kJ mol^{-1} , the hydrogen abstraction should be an inconsequential reaction pathway under the physical conditions, that is, at the collision energy at which the experiment was conducted. Selected TOF spectra are shown in Figure 2 along with the calculated distributions as derived from the forward-convolution fitting routine as described above. A key point to be stressed is that the TOF profiles were successfully replicated with only one product channel with mass combinations of 37 amu (^{11}BCN) and 1 amu (H). The corresponding laboratory angular distribution (LAB) is shown in Figure 3 with the best-fit curve derived from the center-of-mass functions. The LAB distribution is peaked at the center-of-mass angle, but depicts a slightly higher intensity in the forward direction with respect to the atomic boron (^{11}B) beam. The lacking signal at laboratory angles larger than 66° is simply a consequence of the range for the rotatable detector.

4.2. Center of Mass Functions. The center-of-mass angular, $T(\theta)$, and translational energy, $P(E_T)$, distributions as derived for the products of the mass combination 37 amu (^{11}BCN) and 1 amu (H) are shown in Figures 4 and 5, respectively. Let us investigate the center-of-mass translational energy distribution first. For those products that are not internally excited, the reaction energy can be determined by subtracting the collision energy from the maximum translational energy observed. Here, the maximum translational energy, E_{max} , allowed is the arithmetic sum of the collision energy and the absolute of the reaction exoergicity. Accordingly, the reaction exoergicity can be determined by subtracting the collision energy from the maximum translational energy, E_{max} , observed. Within the experimental error limits, this yields a reaction endoergicity of $9 \pm 2 \text{ kJ mol}^{-1}$. This value is in direct agreement to the data derived from our ab initio electronic structure calculations of $8 \pm 4 \text{ kJ mol}^{-1}$ to form the BNC isomer (see Section 5 below).

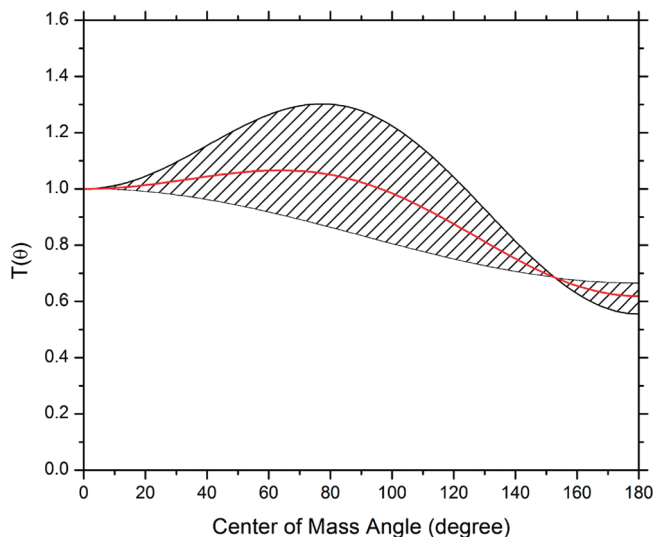


Figure 4. Center-of-mass angular distribution of the boronicyanide product (BNC) observed in the reaction of $^{11}\text{B}(^2\text{P}_j)$ atoms with hydrogen cyanide [$\text{HCN}(X^1\Sigma^+)$] at a collision energy of 29.2 kJ mol^{-1} . The solid red line defines the best fit function while the hatched areas indicate the acceptable upper and lower error limits of the ^{11}BNC product.

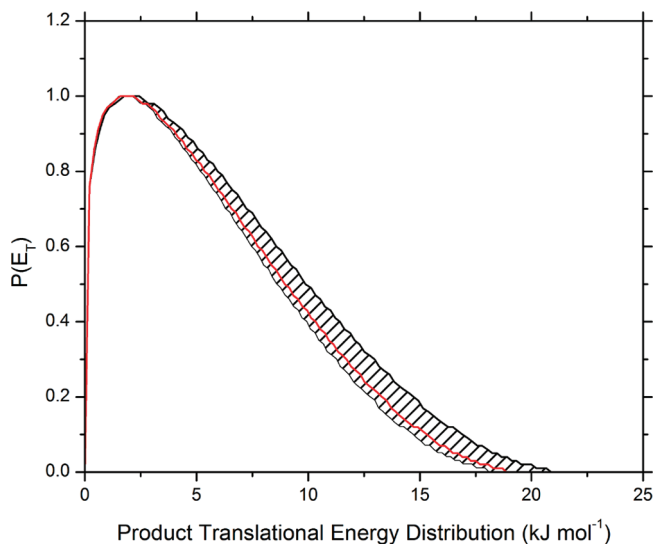


Figure 5. Center-of-mass translational energy flux distribution of the boronicyanide product (^{11}BNC) observed in the reaction of $^{11}\text{B}(^2\text{P}_j)$ atoms with hydrogen cyanide [$\text{HCN}(X^1\Sigma^+)$] at a collision energy of 29.2 kJ mol^{-1} . The solid red line defines the best fit function while the hatched areas indicate the acceptable upper and lower error limits of the ^{11}BNC product.

Second, the translational energy distribution is slightly peaked away from zero translational energy at about $1.5 \pm 0.5 \text{ kJ mol}^{-1}$. This finding indicates—if any—only a small exit barrier involved in the atomic hydrogen loss from a decomposing BHCN intermediate.

The center-of-mass angular distribution reveals important additional information on the reaction dynamics. Upon first inspection, the reader notices that the flux of the center-of-mass angular distribution is always greater than zero for all angles, with an overall forward peaking shape. This finding implies indirect scattering dynamics via a BHCN intermediate. As mentioned earlier, the LAB angular distribution reveals a slight forward scattering preference; this is reflected as well in the center-of-mass angular distribution. An inclination for slight forward scattering can be quantified in the center-of-mass angular distribution by simply taking the ratio of the poles, $I(0^\circ)/$

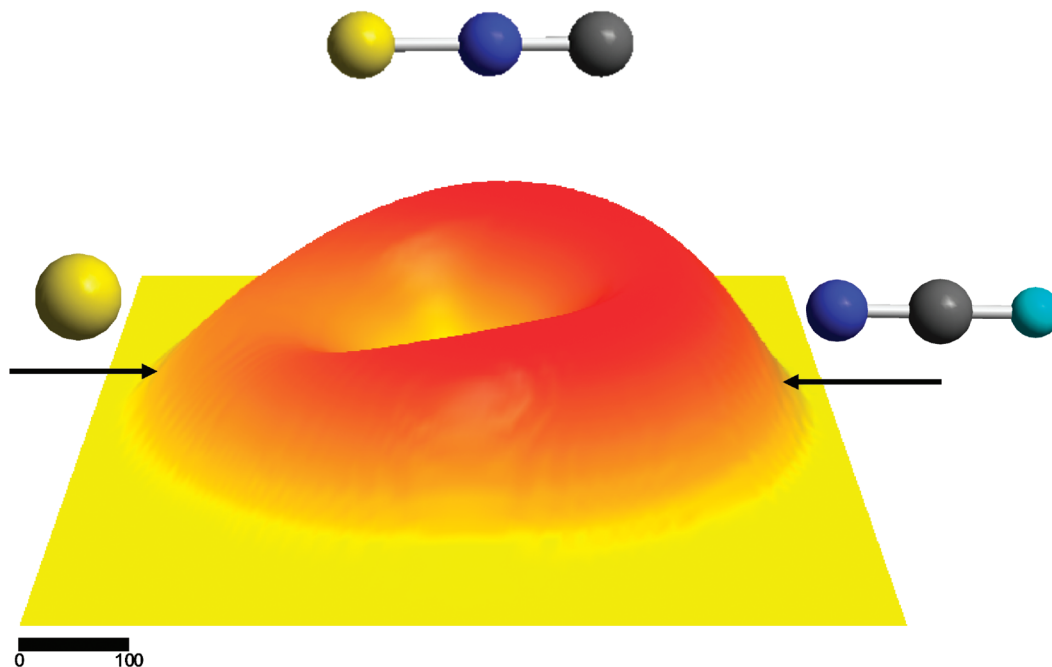


Figure 6. Flux contour map derived from the best fit center-of-mass functions for the boronisocyanide product formed in the reaction of $^{11}\text{B}(^2\text{P}_j)$ atoms with hydrogen cyanide [$\text{HCN}(X^1\Sigma^+)$] at a collision energy of 29.2 kJ mol^{-1} ; the scale is in units of m s^{-1} .

$I(180^\circ) = 1.67 \pm 0.15$ at the collision energy of 29.2 kJ mol^{-1} . Furthermore, the ratio of the poles for the center of mass angular distribution may be used as a molecular clock to estimate the lifetime of the decomposing complex. Also, the forward peaking is only accounted for when the boron atom and the leaving hydrogen atom are situated at opposite sites of the rotation axis of the fragmenting complex. The osculating model relates the intensity ratio at the poles of the center-of-mass angular distribution to τ , the lifetime of the decomposing molecular complex. Here, we calculate a ratio of the lifetime to the rotational period of $0.97^{+0.22}_{-0.14}$; in other words, the lifetime of the decomposing intermediate is about one rotational period. Finally, it should be pointed out that the relatively weak polarization of the center-of-mass angular distributions is likely the result of a small coupling between the initial, \mathbf{L} , and final orbital angular momentum, \mathbf{L}' . Recall, that the magnitude of the final orbital angular momentum \mathbf{L}' is given by $\mu'v_r'b'$, whereas that of \mathbf{L} is given by $\mu v_r b$; where $v_r'v_r$ are the relative velocities and $\mu\mu'$ are the reduced mass of the products and reagents, respectively; and b' and b are the final and initial impact parameters. Due to the leaving light hydrogen atom, μ' is much less than μ . Therefore, angular momentum conservation dictates that most of the initial angular momentum channels into the final rotational angular momentum \mathbf{j}' of the products. Therefore, \mathbf{L} and \mathbf{L}' are only weakly correlated; this gives rise to the slight polarization of the center-of-mass angular distribution⁸⁵ as also observed in the flux contour map of Figure 6.

5. Discussion

Four BNC product isomers have been determined from possible reaction products (Figure 1). Among those—recall that the reaction is endoergic by 8 kJ mol^{-1} —only BNC ($X^1\Sigma^+$) (**p1**) is energetically accessible at our collision energy of 29.2 kJ mol^{-1} . For completeness, we shall briefly discuss the remaining triatomic isomers identified by the ab initio calculations. Boron cyanide [$\text{BCN}(X^1\Sigma^+)$] is the second most stable structure; it lies about 42 kJ mol^{-1} above the linear boronisocyanide isomer. The next stable triatomic species was a cyclic isomer, c-BCN

(X^3A'), formed with a reaction endoergic of 178 kJ mol^{-1} . This species can be seen as an analogue of the isoelectronic cyclic tricarbon molecule, c- C_3 , which also holds a triplet ground state. Finally, the formation carbon boron nitride [$\text{CBN}(X^1\Sigma^+)$] was found to be endoergic by 346 kJ mol^{-1} . Since only the formation of $\text{BNC}(X^1\Sigma^+)$ is energetically feasible, the following discussion focuses on the reaction pathways leading only to this lowest energy structure (**p1**).

A closer look at the BHCN potential energy surface (PES; Figure 7) reveals that the reaction of atomic boron [$\text{B}(^2\text{P}_j)$] with hydrogen cyanide can lead via barrier-less addition processes to three different collision complexes. These intermediates are, with the energy relative to the initial reactants: **i1**, a cyclic $\text{BN}(\text{CH})$ (-193 kJ mol^{-1}) formed via addition of the boron atom to the carbon–nitrogen triple bond; **i2**, an acyclic HCNB isomer (-132 kJ mol^{-1}) via addition of the boron atom to the terminal nitrogen atom lone pair electrons of hydrogen cyanide; and **i3**, an almost trigonal planar BCNH (-49 kJ mol^{-1}) structure, which arose from addition of boron to the carbon atom of hydrogen cyanide. These initial collision complexes can isomerize among each other. The only energetically accessible reaction pathway for **i3** was found to be the ring closure to **i1**. The transition state lies below (-14 kJ mol^{-1}) the energy of the separated reactants. Also, intermediate **i1** and **i2** can isomerize mutually. What is the fate of these collision complexes? Besides isomerization to **i2** as discussed, **i1** can only rearrange to form **i5**. A transition state involved in the isomerization from **i1** to **i6** lies 65 kJ mol^{-1} above the energy of the separated reactants and hence is closed under our experimental conditions considering a collision energy of 29.2 kJ mol^{-1} . Computations show that **i6** can also be accessed from **i4** via a transition state placed 81 kJ mol^{-1} above the energy of the reactants. Therefore, we can safely conclude that **i6** is energetically not accessible in our experiments since both barriers leading to **i6** cannot be overcome. Intermediate **i2** can—besides ring closure to **i1**—decompose via a tight exit transition state to **p1** plus a hydrogen atom; the transition state connecting **i2** to **i7** is too high in energy. Also, the barrier involved in the hydrogen shift

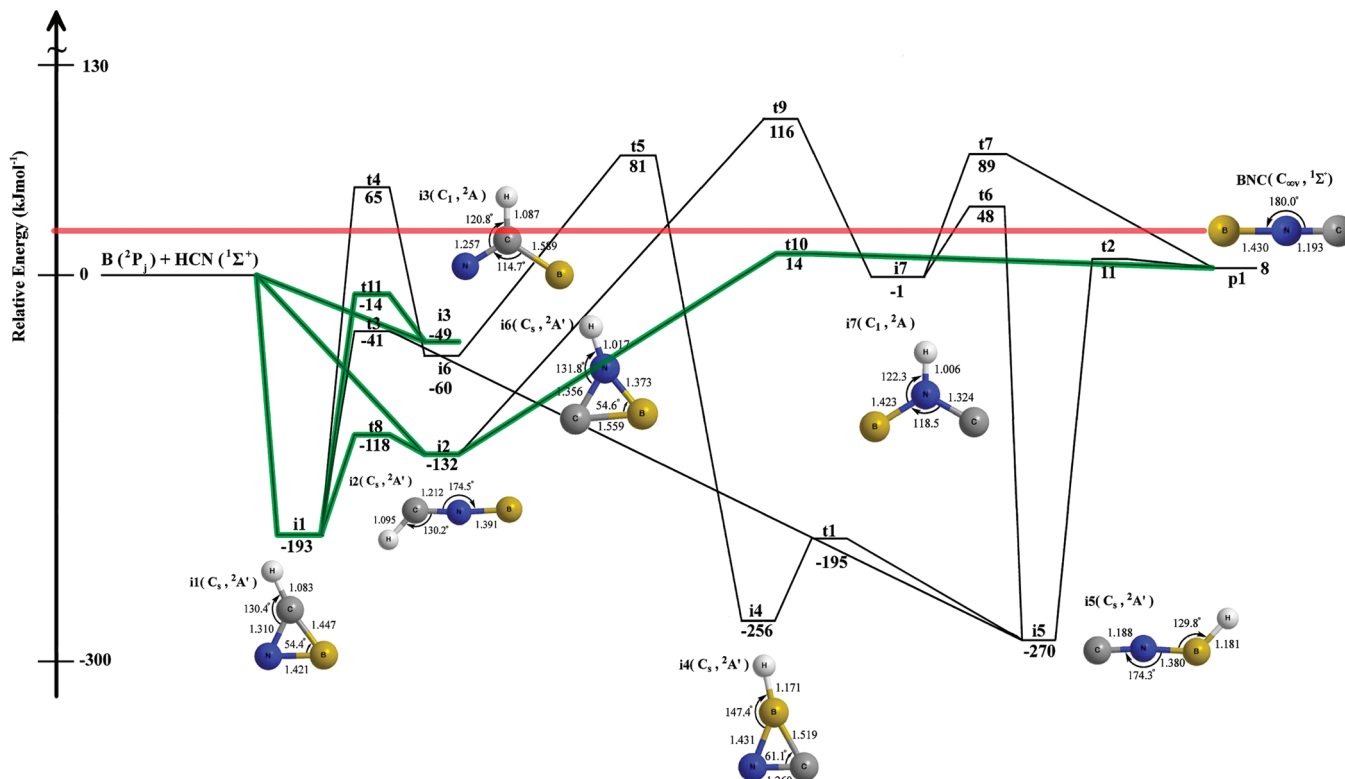


Figure 7. Potential energy surface relevant to the formation of boronisocyanide (**p1**) plus atomic hydrogen. The red line represents the collision energy of 29.2 kJ mol^{-1} ; transition states located above the collision energy are experimentally not accessible in the crossed beams experiments. The green lines present the proposed reaction pathways. Bond lengths are given in units of Angstroms (\AA); bond angles are presented in degrees.

from **i5** to **i7** cannot be overcome. Consequently, intermediate **i7** can be also excluded from the following discussion as well. The remaining structure, **i4**, can only be accessed from **i5**. However, since the only alternative route of **i4** presents an energetically closed route to **i6**, we have to conclude that **i4** could—if at all—only act as an intermediate being involved in the reversible isomerization of **i4** to **i5**. Therefore, this leaves us with intermediates **i1** (rearranging to **i2**), **i2**, and **i5**. Both latter structures can lose a hydrogen atom to form the boronisocyanide product **p1**.

Which is the dominating pathway to form **p1**, $\mathbf{i1} \rightarrow \mathbf{i2} \rightarrow \mathbf{p1} + \text{H}$ or $\mathbf{i1} \rightarrow \mathbf{i5} \rightarrow \mathbf{p1} + \text{H}$? For this, we have to combine the electronic structure calculations with our experimental results. First, recall that the center-of-mass angular distribution depicted flux over the complete angular range as indicative of an indirect reaction mechanism. This indirect or complex forming reaction mechanism is fully supported by our electronic structure calculations as both feasible routes $\mathbf{i1} \rightarrow \mathbf{i2} \rightarrow \mathbf{p1} + \text{H}$ and $\mathbf{i1} \rightarrow \mathbf{i5} \rightarrow \mathbf{p1} + \text{H}$ involve bound intermediates. Further, the experimentally observed forward peaking in the center-of-mass angular and flux distribution depicts a ratio of the poles greater than one; this suggests the existence of an osculating $^{11}\text{BCNH}$ complex. This forward scattering can only arise if the departing hydrogen atom and the incorporated boron atom are located on opposite sites of the rotational axis. Since boron isocyanide is linear, it can only be excited to B-like rotations. A close look at intermediates **i2** and **i5** suggests that only intermediate **i2** fulfills this requirement. Therefore, we can conclude that **i2** decomposes to **p1** plus atomic hydrogen via a rather loose exit transition state located only a few kJ mol^{-1} above the energy of the separated products. Since both **i2** and **i5** originate from an isomerization of **i1**, it is sensible to analyze the inherent isomerization barriers. Here, the barrier involved in the isomer-

ization to **i2** lies 97 kJ mol^{-1} above **i1**, whereas the transition state connecting **i1** and **i5** resides higher in energy, that is, 152 kJ mol^{-1} above **i1**. Therefore, based on the energetics of the transition states, intermediate **i1** should preferentially isomerize to **i2**, which in turn forms boronisocyanide plus atomic hydrogen. Consequently, both the experimental and theoretical findings correlate exceptionally well and clearly demonstrate that the boronisocyanide molecule is formed via a barrier-less addition involving two possible intermediates, **i1** and **i2**, which can isomerize. An ultimate hydrogen loss of **i2** yields the desired product isomer. No other product isomer can be formed in this reaction due to the unfavorable energetics of these reactions.

Considering that acetylene [$\text{C}_2\text{H}_2(\text{X}^1\Sigma_g^+)$] and hydrogen cyanide [$\text{HCN}(\text{X}^1\Sigma^+)$] are isoelectronic, save for the inversion symmetry, and that the reaction dynamics of boron with acetylene have been reported previously,^{8,86,87} a brief description of the similarities and differences will be given here. First, both reactions are initiated by a barrier-less addition of atomic boron to the highly unsaturated triple bond forming long-lived and stabilized (-193 kJ mol^{-1} , HBCN) and (-297 kJ mol^{-1} , HCBCN) cyclic intermediates. Also, both angular distributions in the center of mass frame show flux over the complete angular range and reveal a slight forward peaking constantly above zero. These observations are suggestive of indirect scattering dynamics along with the incorporated boron atom and leaving hydrogen atom being located on opposite sides of the rotation axis of the fragmenting intermediate. Indeed, the ab initio results correlate well with these experimental observations as both involve reaction paths with multiple cyclic intermediates coupled with hydrogen migration and finally ring-opening. Perhaps the most distinctive difference between these two reactions is the discovery of a cyclic product $\text{c-BC}_2\text{H}(\text{X}^2\text{A}')$ from the ground state reaction of atomic boron with acetylene which arose from

a direct hydrogen elimination of the cyclic intermediate or an isomerization of the linear product. Our electronic structure calculations did reveal a cyclic BNC (X^3A') isomer as a possible product; however the calculated reaction endoergicity of 177 kJ mol⁻¹ was well beyond the constraints of the experimental conditions. Also, no pathway was discovered in which the cyclic product [BNC (X^3A')] could have been formed from an isomerization of the linear [BNC ($X^1\Sigma^+$)] product.

6. Conclusions

We have conducted a crossed molecular beam experiment of atomic boron [B(2P_j)] and hydrogen cyanide [HCN($X^1\Sigma^+$)] at a collision energy of 29.2 kJ mol⁻¹. The results represent the very first directed gas phase synthesis of the boronocyanide [BNC($X^1\Sigma^+$)] molecule, which is isoelectronic with the well-known tricarbon molecule; we also collected valuable information on the reaction dynamics. A comparison of the experimental data with the theoretical investigation elucidated a reaction pathway leading to the experimentally observed linear boronocyanide product. Upon collision, the electrophilic boron atom may add to the hydrogen cyanide molecule forming three collision complexes **i1**–**i3**. The ultimate fate of these complexes is their isomerization to **i2**, which in turn decomposed via a rather loose exit transitions state to form the linear boronocyanide molecule. The overall reaction was shown to be endoergic by 9 ± 2 kJ mol⁻¹; this corresponds very well with the theoretical value of 8 ± 4 kJ mol⁻¹. These findings and the first directed synthesis of boronocyanide hold important implications to rationalize the formation and electronic properties of isoelectronic molecules such as CCC and BNC—the simplest triatomic molecule with three distinct, neighboring main group atoms of the second row of the periodic table of the elements, boron, carbon, and nitrogen. Finally, we would like to note that the detection of the boronocyanide molecule has also potential astrophysical implications as this molecule could be present in the Orion-KL nebula.

Acknowledgment. This work was supported by the Air Force Office of Scientific Research (A9550-09-1-0177) (PM, RIK). B. J. thanks the NASA Postdoctoral Program at the NASA Astrobiology Institute, administered by Oak Ridge Associated Universities.

References and Notes

- (1) Aihara, J.-i.; Kanno, H.; Ishida, T. *J. Am. Chem. Soc.* **2005**, *127*, 13324.
- (2) Bower, J. G. *Progr. Boron Chem.* **1970**, *2*, 231.
- (3) Lappert, M. F. *Chem. Boron Its Compd.* **1967**, 443.
- (4) Muetterties, E. L. *Chem. Boron Its Compd.* **1967**, 1.
- (5) Niedenzu, K.; Dawson, J. W. *Chem. Boron Its Compd.* **1967**, 377.
- (6) Noeth, H. *Progr. Boron Chem.* **1970**, *3*, 211.
- (7) *Contemporary Boron Chemistry*; Royal Society of Chemistry: Cambridge, 2000.
- (8) Balucani, N.; Zhang, F.; Kaiser, R. I. *Chem. Rev.* **2010**, *ACS ASAP*.
- (9) Conley, B. L.; Williams, T. J. *J. Am. Chem. Soc.*, *132*, 1764.
- (10) Hase, Y. *Spectrochim. Acta, Part A*, *75*, 461.
- (11) Saloni, J.; Kolodziejczyk, W.; Roszak, S.; Majumdar, D.; Hill, G., Jr.; Leszczynski, J. *J. Phys. Chem. C*, *114*, 1528.
- (12) Tai, T. B.; Grant, D. J.; Nguyen, M. T.; Dixon, D. A. *J. Phys. Chem. A*, *114*, 994.
- (13) Tai, T. B.; Nguyen, M. T.; Dixon, D. A. *J. Phys. Chem. A*, *ACS ASAP*.
- (14) Abad, M. D.; Caceres, D.; Pogozhev, Y. S.; Shtansky, D. V.; Sanchez-Lopez, J. C. *Plasma Processes Polym.* **2009**, *6*, S107.
- (15) Chen, Y.; Yang, S.; Zhang, J. *Surf. Interface Anal.* **2009**, *41*, 865.
- (16) Foroutan-Nejad, C.; Rashidi-Ranjbar, P. *THEOCHEM* **2009**, *901*, 243.
- (17) Gao, S.; Wu, W.; Mo, Y. *J. Phys. Chem. A* **2009**, *113*, 8108.
- (18) Ilyin, A. P.; Tolbanova, L. O.; Mostovschikov, A. V. *Wiss. Ber. — Forschungszent. Karlsruhe* **2009**, *34*.
- (19) Oganov, A. R.; Solozhenko, V. L. *Sverkhverd. Mater.* **2009**, *3*.
- (20) Wade, K. *Nat. Chem.* **2009**, *1*, 92.
- (21) Zhang, L.; Ying, F.; Wu, W.; Hiberty, P. C.; Shaik, S. *Chem.—Eur. J.* **2009**, *15*, 2979.
- (22) Zope, R. R. *Epl* **2009**, *85*, 68005/1.
- (23) Langmuir, I. *J. Am. Chem. Soc.* **1919**, *41*, 868.
- (24) Rayner-Canham, G. *Found. Chem.* **2009**, *11*, 123.
- (25) Martin, J. M. L.; Taylor, P. R. *J. Phys. Chem.* **1994**, *98*, 6105.
- (26) Lanzisera, D. V.; Andrews, L.; Taylor, P. R. *J. Phys. Chem. A* **1997**, *101*, 7134.
- (27) Fueno, H.; Taniguchi, Y. *Chem. Phys. Lett.* **1999**, *312*, 65.
- (28) Mebel, A. M.; Kaiser, R. I. *Chem. Phys. Lett.* **2002**, *360*, 139.
- (29) Han, W.-Q.; Mickelson, W.; Cumings, J.; Zettl, A. *Appl. Phys. Lett.* **2002**, *81*, 1110.
- (30) Caretti, I.; Jiménez, I.; Gago, R.; Cáceres, D.; Abendroth, B.; Albella, J. M. *Diamond Relat. Mater.* **2004**, *13*, 1532.
- (31) Guo, X.; Liu, Z.; Luo, X.; Yu, D.; He, J.; Tian, Y.; Sun, J.; Wang, H.-T. *Diamond Relat. Mater.* **2007**, *16*, 526.
- (32) Caretti, I.; Albella, J. M.; Jiménez, I. *Diamond Relat. Mater.* **2007**, *16*, 63.
- (33) Andrews, L.; Hassanzadeh, P.; Burkholder, T. R.; Martin, J. M. L. *J. Chem. Phys.* **1993**, *98*, 922.
- (34) Chattopadhyay, S.; Chien, S. C.; Chen, L. C.; Chen, K. H.; Lee, H. Y. *Diamond Relat. Mater.* **2002**, *11*, 708.
- (35) Ugarov, M. V.; Ageev, V. P.; Karabutov, A. V.; Loubnin, E. N.; Pimenov, S. M.; Konov, V. I.; Bensaoula, A. *Appl. Surf. Sci.* **1999**, *138–139*, 359.
- (36) Shimada, Y.; Chikamatsu, K.; Kimura, C.; Aoki, H.; Sugino, T. *Appl. Surf. Sci.* **2006**, *253*, 1459.
- (37) Ying, Z. F.; Yu, D.; Ling, H.; Xu, N.; Lu, Y. F.; Sun, J.; Wu, J. D. *Diamond Relat. Mater.* **2007**, *16*, 1579.
- (38) Ma, S.; Chen, X. Method for manufacturing BCN hard coating with good anti-frictional and abrasion-resistant performances. The Peoples Republic of China, 2009; Vol. CN 101525734.
- (39) Terrones, M.; Grobert, N.; Terrones, H. *Carbon* **2002**, *40*, 1665.
- (40) Golberg, D.; Dorozhkin, P. S.; Bando, Y.; Dong, Z. C.; Tang, C. C.; Uemura, Y.; Grobert, N.; Reyes-Reyes, M.; Terrones, H.; Terrones, M. *Appl. Phys. A: Mater. Sci. Process.* **2003**, *76*, 499.
- (41) Sakakihara, M.; Ichinose, Y.; Yamaguchi, S. *Nippon Kinzoku Gakkaishi* **1992**, *56*, 459.
- (42) Wu, H. Y.; Fan, X. F.; Kuo, J.-L.; Deng, W.-Q. *Chem. Commun.* **2010**, *46*, 883.
- (43) Cunha, K.; Lambert, D. L.; Lemke, M.; Gies, D. R.; Roberts, L. C. *The Astrophysical Journal* **1997**, *478*, 211.
- (44) Jura, M.; Meyer, D. M.; Hawkins, I.; Cardelli, H. A. *Astrophys. J.* **1996**, *456*, 598.
- (45) Hawk, J. C.; Sembach, K. R.; Savage, B. D. *Astrophys. J.* **2000**, *543*, 278.
- (46) Ritchey, A. M.; Federman, S. R.; Sheffer, Y.; Lambert, D. L. Boron Abundances in Diffuse Interstellar Clouds, 2009.
- (47) Cunha, K.; Smith, V. V.; Parizot, E.; Lambert, D. L. *Astrophys. J.* **2000**, *543*, 850.
- (48) Lambert, D. L.; Sheffer, Y.; Federman, S. R.; Cardelli, J. A.; Sofia, U. J.; Knauth, D. C. *Astrophys. J.* **1998**, *494*, 614.
- (49) Schilke, P.; Benford, D. J.; Hunter, T. R.; Lis, D. C.; Phillips, T. G. *Astrophys. J. Suppl. Ser.* **2001**, *132*, 281.
- (50) Redlich, P.; Loeffler, J.; Ajayan, P. M.; Bill, J.; Aldinger, F.; Rühle, M. *Chem. Phys. Lett.* **1996**, *260*, 465.
- (51) Weng-Sieh, Z.; Cherrey, K.; Chopra, N. G.; Blase, X.; Miyamoto, Y.; Rubio, A.; Cohen, M. L.; Louie, S. G.; Zettl, A.; Gronsky, R. *Phys. Rev. B* **1995**, *51*, 11229.
- (52) Stephan, O.; Ajayan, P. M.; Colliex, C.; Redlich, P.; Lambert, J. M.; Bernier, P.; Lefin, P. *Science* **1994**, *266*, 1683.
- (53) Moriyoshi, Y.; Shimizu, Y.; Watanabe, T. *Thin Solid Films* **2001**, *390*, 26.
- (54) Laidani, N.; Anderle, M.; Canteri, R.; Elia, L.; Luches, A.; Martino, M.; Micheli, V.; Speranza, G. *Appl. Surf. Sci.* **2000**, *157*, 135.
- (55) Zhang, Y.; Gu, H.; Suenaga, K.; Iijima, S. *Chem. Phys. Lett.* **1997**, *279*, 264.
- (56) Lanzisera, D. V.; Andrews, L. *J. Phys. Chem. A* **1997**, *101*, 824.
- (57) Yu, J.; Bai, X. D.; Ahn, J.; Yoon, S. F.; Wang, E. G. *Chem. Phys. Lett.* **2000**, *323*, 529.
- (58) Bill, J.; Reidel, R. Z. *Anorg. Allg. Chem.* **1992**, *610*, 83.
- (59) Zhi, C. Y.; Bai, X. D.; Wang, E. G. *Appl. Phys. Lett.* **2002**, *80*, 3590.
- (60) Zhang, H. R.; Liang, E. J.; P., D.; Du, Z. L.; Guo, X. Y. *Acta Phys. Sin -CH ED* **2002**, *51*, 2901.
- (61) Terrones, M.; Benito, A. M.; Manteca-Diego, C.; Hsu, W. K.; Osman, O. I.; Hare, J. P.; Reid, D. G.; Terrones, H.; Cheetham, A. K.; Prassides, K.; Kroto, H. W.; Walton, D. R. M. *Chem. Phys. Lett.* **1996**, *257*, 576.

- (62) Kohler-Redlich, P.; Terrones, M.; Manteca-Diego, C.; Hsu, W. K.; Terrones, H.; Rühle, M.; Kroto, H. W.; Walton, D. R. M. *Chem. Phys. Lett.* **1999**, *310*, 459.
- (63) Blank, V. D.; Seepujak, A.; Polyakov, E. V.; Batov, D. V.; Kulnitskiy, B. A.; Parkhomenko, Y. N.; Skryleva, E. A.; Bangert, U.; Gutiérrez-Sosa, A.; Harvey, A. J. *Carbon* **2009**, *47*, 3167.
- (64) Nakao, S.; Sonoda, T.; Tsugawa, K.; Choi, J.; Kato, T. *Vacuum* **2009**, *84*, 642.
- (65) Essafti, A.; Ech-Chamikh, E.; Azizan, M.; Ijdiyaou, Y. *Phys. Chem. News* **2009**, *48*, 30.
- (66) Van Orden, A.; Saykally, R. J. *Chem. Rev.* **1998**, *98*, 2313.
- (67) Guo, Y. G., X.; Kaiser, R. I. *Int. J. Mass Spec.* **2006**, *249/250*, 420.
- (68) Guo, Y.; Gu, X.; Kawamura, E.; Kaiser, R. I. *Rev. Sci. Instrum.* **2006**, *77*, 034701/1.
- (69) Gu, X.; Guo, Y.; Kaiser, R. I. *Int. J. Mass Spec.* **2005**, *246*, 29.
- (70) Gu, X. G., Y.; Kawamura, E.; Kaiser, R. I. *J. Vac. Sci. Technol. A* **2006**, *24*, 505.
- (71) Proch, D.; Trickl, T. *Rev. Sci. Instrum.* **1989**, *60*, 713.
- (72) Vernon, M., University of California, 1981.
- (73) Weiss, M. S., University of California, 1986.
- (74) Levine, R. D. *Molecular Reaction Dynamics*; Cambridge University Press: Cambridge, U.K., 2005.
- (75) Becke, A. D. *J. Chem. Phys.* **1992**, *96*, 2155.
- (76) Becke, A. D. *J. Chem. Phys.* **1992**, *92*.
- (77) Becke, A. D. *J. Chem. Phys.* **1993**, *98*, 5648.
- (78) Lee, C.; Yang, W.; Parr, R. G. *Phys. Rev. B* **1988**, *37*, 785.
- (79) Purvis, G. D.; Bartlett, R. J. *J. Chem. Phys.* **1982**, *76*, 1910.
- (80) Hampel, C.; Peterson, K. A.; Werner, H.-J. *Chem. Phys. Lett.* **1992**, *190*, 1.
- (81) Knowles, P. J.; Hampel, C.; Werner, H.-J. *J. Chem. Phys.* **1994**, *99*, 5219.
- (82) Deegan, M. J. O.; Knowles, P. J. *Chem. Phys. Lett.* **1994**, *277*, 321.
- (83) Frisch, M. J.; Trucks, G. W.; Schlegel, H. B.; Scuseria, G. E.; Robb, M. A.; Cheeseman, J. R.; Montgomery, J. A.; T. V.; Jr., Kudin, K. N.; Burant, J. C.; Millam, J. M.; Iyengar, S. S.; Tomasi, J.; Barone, V.; Mennucci, B.; Cossi, M.; Scalmani, G.; Rega, N.; Petersson, G. A.; Nakatsuji, H.; Hada, M.; Ehara, M.; Toyota, K.; Fukuda, R.; Hasegawa, J.; Ishida, M.; Nakajima, T.; Honda, Y.; Kitao, O.; Nakai, H.; Klene, M.; Li, X.; Knox, J. E.; Hratchian, H. P.; Cross, J. B.; Bakken, V.; Adam, C.; Jaramillo, J.; Gomperts, R.; Stratmann, R. E.; Yazyev, O.; Austin, A. J.; Cammi, R.; Pomelli, C.; Ochterski, J. W.; Ayala, P. Y.; Morokuma, K.; Voth, G. A.; Salvador, P.; Dannenberg, J. J.; Zakrzewski, V. G.; Dapprich, S.; Daniels, A. D.; Strain, M. C.; Farkas, O.; Malick, D. K.; Rabuck, A. D.; Raghavachari, K.; Foresman, J. B.; Ortiz, J. V.; Cui, Q.; Baboul, A. G.; Clifford, S.; Cioslowski, J.; Stefanov, B. B.; G. Liu, A. L.; Piskorz, P.; Komaromi, I.; Martin, R. L.; Fox, D. J.; Keith, T.; Al-Laham, M. A.; Peng, C. Y.; Nanayakkara, A.; Challacombe, M.; Gill, P. M. W.; Johnson, B.; Chen, W.; Wong, M. W.; Gonzalez, C.; Pople, J. A.; *Gaussian 03 Revision C.02*; Gaussian, Inc.: Wallingford, 2004.
- (84) National Institute of Standards and Technology, NIST G. M. Chemistry WebBook. In *NIST Standard Reference Database Number 69*; Linstrom, P. J., Mallard, W. G., Ed.
- (85) Kaiser, R. I.; Mebel, A. M. *Intl. Rev. Phys. Chem.* **2002**, *21*, 307.
- (86) Kaiser, R. I.; Balucani, N.; Galland, N.; Caralp, F.; Rayez, M. T.; Hannachi, Y. *Phys. Chem. Chem. Phys.* **2004**, *6*, 2205.
- (87) Zhang, F.; Gu, X.; Kaiser, R. I.; Bettinger, H. *Chem. Phys. Lett.* **2008**, *450*, 178.

JP104426F